

Miniature Submarine using Near-Infrared Spectroscopy to Detect and Collect Microplastics

Brandon Pae, Darson Chen

Horace Mann School, 231 W 246th St, Bronx, NY, 10471, USA; brandon.pae@gmail.com

ABSTRACT: A promising solution to detecting and collecting ocean microplastics is utilizing near-infrared (NIR) spectroscopy. NIR spectroscopy is a cost-effective, safe, and accurate method to determine the chemical composition of unknown materials. However, since it cannot easily function underwater as light cannot penetrate the ocean surface, a submarine drone design developed here will employ near-infrared spectroscopy to differentiate the collected micro-objects. In particular, an experiment was conducted where varying sizes of kombu (edible kelp) and microplastics were scanned by a NIR spectrometer to determine the mass composition of a given sample. A least sum of squares method was used to analyze the spectra data from an unknown concentration of microplastics by comparing the spectra data to stored spectra datasets which were produced from samples of known concentrations. The results showed that least squares analysis was a generally effective method to compare such spectra graphs and deduce the mass composition of a given sample. Although, more improvements including the analysis of the spectra graph's curvature and an increased amount of composition data, are necessary to make the approach more accurate.

KEYWORDS: Materials Science; Computation and Theory; NIR Spectroscopy; R Programming; Least squares Analysis.

■ Introduction

Ocean plastic pollution, which consists of harmful macro and microplastics, is a dire issue that the scientific community must solve. Marine organisms easily mistake microplastics, which are under 5 mm, for food and become polluted, threatening other creatures, like humans, that consume them.¹ Additionally, since microplastics are broken off from macroplastics, they pollute the ocean the same way macroplastics do; stains on microplastics still react in the water to form toxic chemicals. These chemicals can spread anywhere in the ocean as microplastics exist in all ocean depths.²

Unfortunately, current solutions to ocean plastic pollution mainly target macroplastics on the ocean surface, which does not address the prevalent microplastic problem. These solutions include the Ocean Cleanup's Interceptor that collects large pieces of plastic and the ESA satellites that detect macroplastics on the ocean surface.³ There are also reactions and chemicals that have been developed to clean plastics, including ferromagnetic materials, but they cannot be effectively utilized in the ocean environment due to its vast area.

Additionally, there are currently various chemometric techniques that are used to analyze sample compositions with spectroscopy. In particular, a widely used method is the Beer-Lambert Law, which relates the amount of absorption to material concentration.⁴ However, one major limitation of this method is that it does not utilize reflectance measurements, which many spectrometers use. The Beer-Lambert Law also requires an optical density coefficient. This coefficient is dependent on the materials in the given sample and must be known in order to execute the chemometric analysis.⁴ As a result, if the materials in the given sample are unknown, then their optical density coefficients are also unknown, and the analysis cannot be executed.

One promising solution to detecting and collecting ocean microplastics is NIR reflectance spectroscopy.⁵ It is cost-effective, safe, and accurate in determining the chemical composition of unknown materials.⁶ However, while the aforementioned ESA satellites utilize NIR light to detect macroplastics, they cannot detect microplastics on the ocean surface because they are too far from the ocean. Furthermore, these satellites cannot detect the widespread ocean microplastics beneath the ocean surface because NIR light cannot penetrate water.

Besides NIR reflectance spectroscopy, Raman spectroscopy can be used for a similar experiment. Raman spectroscopy is a non-destructive technique that gives a chemical analysis of an object. The molecular interaction and chemical structure of a molecule can be identified, making Raman spectroscopy a viable alternative for determining microplastics due to their unique chemical makeup. Moreover, the spectroscopy technique is fundamentally researched and experimented with. However, Raman spectra present units primarily in 1/cm instead of on the micro or nanoscale, making the graph analysis more challenging. Additionally, due to microplastics at times being mixed with toxic chemicals as well as other substances, it is not clear how these possible extra substances may affect or alter the Raman signal and data due to the impurity of the microplastic.

Even with NIR reflectance spectroscopy, an analysis of the intensity peaks of the respective spectra graphs could determine whether a substance contained plastic or not. The peak intensity of a spectra is created by the unique molecule composition of a substance, and a plastic may consistently give a peak intensity that can be read through a machine learning system. Nonetheless, this option was not chosen due to the machine learning algorithm required to analyze the peak in

tensities. The algorithm would require extra time to code that the chosen method did not need.

This experiment endeavors to capture the microplastics using NIR reflectance spectroscopy. NIR spectroscopy is employed inside a submarine drone, which is an isolated system without water where NIR light can function. Even if there is no air in the submarine, NIR light would still be able to travel through the vacuum.

The NIR spectroscopy within a submarine drone is highly significant as it opens the possibility of detecting and identifying ocean microplastics autonomously, efficiently, and harmlessly. Due to the detection, the submarine drone can intake the microplastics, leading to a reduced amount of plastic pollution. In addition, the application of the least squares algorithm to compare resulting spectra graphs is a novel and less computationally intensive method to determine the mass composition of a given plastic and algae sample. This method first stores the spectra of samples with known concentrations and then compares the stored graph with new spectra graphs from new test concentrations to find the closest matches. The near-infrared reflectance spectroscopy within a submarine drone could efficiently differentiate the collected microplastics from small pieces of kombu using a least squares analysis method.

■ Methods

The following materials were used in the experiment: sheets of Polyethylene Terephthalate (PET) and Low-Density Polyethylene (LDPE), kombu (edible algae), a Texas Instruments NIR spectrometer, NIR protective glasses, disposable gloves, protective goggles, a precision scale, a ruler, a stand, a computer with NanoScan installed, scissors, and paper plates. To set up the experiment, the NIR spectrometer was attached to a ruler via tape, so the spectrometer's scan window faced downwards (as pictured in Figure 1; all images are shown on pages 3-5). A ruler was attached to a stand which was then adjusted so the spectrometer's scan window was 1.5 mm away from the floor (as pictured in Figure 1). A spectrometer was connected to a computer in order to send the reflectance data to the NanoScan application. Before preparing the microplastics, the disposable gloves and protective eyewear were worn. The microplastics were made by cutting over 100 pieces of PET, LDPE, and kombu with lengths under 5 mm (as pictured in Figure 3). Afterward, a circular paper plate was cut to have a small rectangle with dimensions 7.5 mm by 3 mm drawn in the center. Next, the data tables (on page 7) were made to record given mass values.

Starting data collection, a piece of kombu that exactly covered the previously drawn rectangle was cut. It was weighed on the precision scale (as pictured in Figure 2) and its mass was recorded. The kombu piece was then placed on the drawn rectangle and slid under the spectrometer so that the kombu was directly under the scan window (as pictured in Figure 4). Before the NIR spectrometer was activated, NIR-protective goggles were worn. The spectrometer was activated, and light shone on the sample (as pictured in Figure 5). Once the reflectance data was sent to the computer and stored in a .csv file, the process with the kombu (cutting,

weighing, and scanning it) was repeated with pieces of PET and LDPE that similarly covered the drawn rectangle.

Afterwards, a piece of PET was cut that covered half of the drawn rectangle, and another piece of LDPE was cut that covered the rectangle's remaining half. Their masses were weighed and recorded, and the NIR scanning process was repeated. Then, pieces of PET, LDPE, and kombu were cut such that they each covered about $\frac{1}{3}$ of the drawn rectangle (as pictured in Figure 6). The weighing and scanning process was then repeated with this sample. Finally, a piece of PET that covered $\frac{1}{4}$ of the rectangle and a piece of kombu that covered $\frac{3}{4}$ of the rectangle were cut and the rest of the data collection process was repeated.

Afterward, a very similar process was repeated to collect the values shown in the second data table. However, instead of uniform macro pieces (as pictured in Figure 6), the small bits of plastic and kombu (< 5 mm) were used instead (as pictured in Figure 7). In addition, in these trials the materials were not separated but instead mixed together (as pictured in Figure 8). However, the approximate ratios of each material in each trial (e.g., LDPE covering $\frac{1}{3}$ of the drawn rectangle) were maintained. After this data collection was finished, the disposable gloves, microplastics, and kombu were disposed of within the garbage.

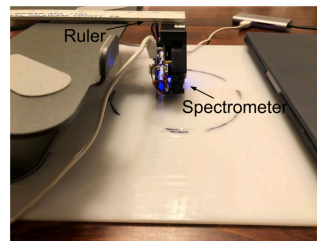


Figure 1: Making the setup.

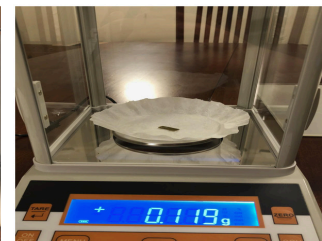


Figure 2: Weighing the kombu.



Figure 3: Cutting the PET, LDPE, and kombu.



Figure 4: Sample under the spectrometer.



Figure 5: Activating the NIR spectrometer.



Figure 6: Making a sample that is $\frac{1}{3}$ PET, $\frac{1}{3}$ LDPE, and $\frac{1}{3}$ kombu.

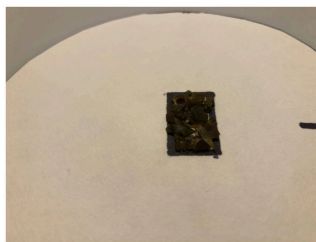


Figure 7: Making a sample with small pieces of kombu.

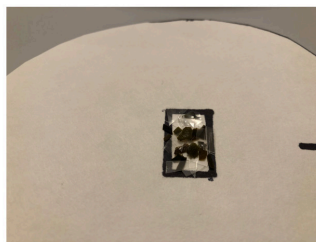
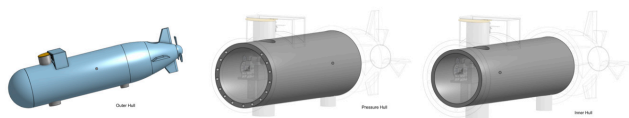


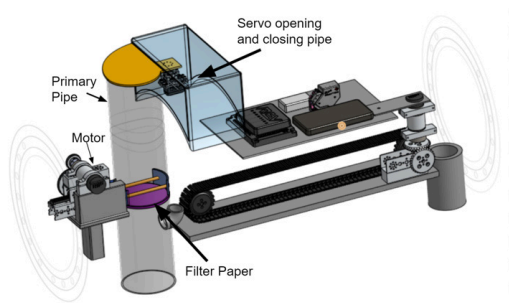
Figure 8: Making sample of small mixed pieces of plastic and kombu.

Engineering Design:

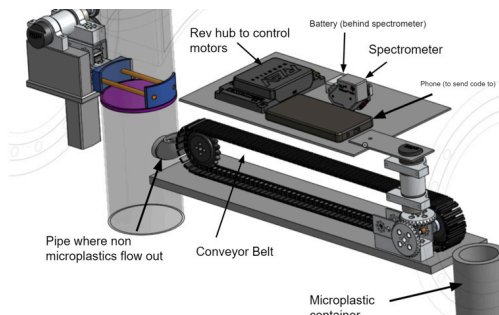
This is a computer aided model of a hypothetical submarine drone to collect microplastics. The drone design consists of an outer hull, an inner hull, and a pressure hull in between the two that holds the water and air. The water and air determine the depth the drone will go in the ocean.



The machinations inside include a pipe that moves the micro-objects outside onto a filter paper where the water passes through, leaving the micro-objects on the filter paper. A motor pushes the micro-objects through while a servo on top of the drone closes the pipe to block water from entering and touching the machines.



Micro-objects are pushed onto the conveyor belt that moves them under the spectrometer to be scanned. The scan determines whether they are microplastics or not. If the sample is not more than 10% microplastics, the conveyor belt reverses and drops everything down a pipe that is connected back to the first pipe where the water is flowing out. If there are sufficient microplastics, they will be dropped into the microplastic container.



Data Analysis:

The R programming language was used in RStudio. The spectrometer returned information on the percentage of each wavelength, from 900 to 1700 nm, that is reflected from the sample. Therefore, after preparing samples of the kombu and microplastics with known mass concentrations of microplastics and obtaining the spectra data, the information was organized into a data table with the wavelength as the independent variable and the reflectance value as the dependent variable. After conducting multiple trials, spectra graphs were generated that represented various compositions (e.g., 50% plastics, 50% kombu).

Afterward, multiple samples were created with different concentrations of microplastics. After recording the reflectance values from these six new test samples and producing spectra graphs accordingly, it was determined which previous spectra graph (from the initial six trials) best represented the new test graph in question. To quantify the best fit, a least sum of squares approach was utilized, such that the difference between the two spectra graphs (the test graph and an initial spectra graph) for each wavelength was squared and summed together. After completing the analysis between the given test graph and each of the initial six graphs, the initial spectra graph that produced the smallest sum of squares value (which means that it has the highest similarity to the given test graph) was chosen. Since this initial spectra graph was produced from a known concentration of PET, LDPE, and kombu, the associated concentrations were also used to indicate the concentrations of the test graph in question.

The full code developed for this experiment can be found in a GitHub Repository:

<https://github.com/paeb/ISEF-Code>.

Data Tables:

In Table 1, the mass of PET, LDPE, and Kombu in each sample were recorded to calculate the sample's unique mass composition. The compositions were used to identify the respective NIR spectra graphs.

Table 1: First set of trials (stored cases).

PET Mass (g)	LDPE Mass (g)	Kombu Mass (g)	Total Mass (g)	PET Percent Mass (%)	LDPE Percent Mass (%)	Kombu Percent Mass (%)
0	0	0.393	0.393	0	0	100
0.073	0	0	0.073	100	0	0
0	0.033	0	0.033	0	100	0
0.038	0.013	0	0.051	75	25	0
0.024	0.008	0.118	0.15	16	5	79
0.021	0	0.116	0.137	15	0	85

In Table 2 the trials contained the samples which were cut up and mixed. Then the mass of the PET, LDPE, and Kombu in each sample were recorded to calculate the sample's unique mass composition for the respective NIR spectra graph.

Table 2: Second set of trials (test cases).

PET Mass (g)	LDPE Mass (g)	Kombu Mass (g)	Total Mass (g)	PET Percent Mass (%)	LDPE Percent Mass (%)	Kombu Percent Mass (%)
0	0	0.258	0.258	0	0	100
0.077	0	0	0.077	100	0	0
0	0.017	0	0.017	0	100	0
0.044	0.012	0	0.056	79	21	0

0.044	0.012	0	0.056	79	21	0
0.033	0.008	0.077	0.118	28	7	65
0.018	0	0.167	0.185	10	0	90

■ Results and Discussion

In analyzing the results, certain compositions were accurately compared from the least squares algorithm, while others were not. In particular, the spectra graphs from the test samples (from the second set of trials) in Figure 8 (0% PET, 0% LDPE, and 100% kombu), Figure 9 (0% PET, 100% LDPE, and 0% kombu), and Figure 10 (10% PET, 0% LDPE, and 90% kombu) fit very closely with the spectra graphs from the first stored trials that have the most similar mass percentages. There was not an exact match in composition for Figure 10 because there was no composition from the first set of trials that had 10% PET and 90% kombu; however, the closest composition from the first set of trials (0% PET and 100% kombu) was accurately matched as the closest spectra graph.

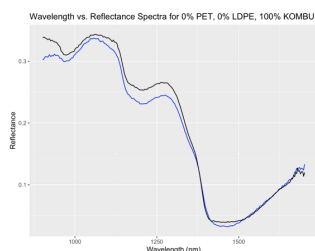


Figure 8: 0% PET, 0% LDPE, 100% KOMBU best fits the spectra graph of: 0% PET, 0% LDPE, 100% KOMBU; peak intensity in the 1150 nm range. The NIR spectrometer can accurately detect 100% KOMBU substances.

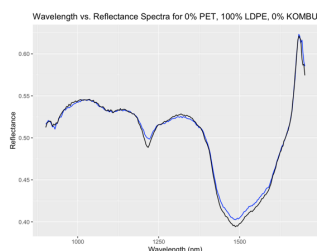


Figure 9: 0% PET, 100% LDPE, 0% KOMBU best fits the spectra graph of: 0% PET, 100% LDPE, 0% KOMBU; peak intensity in the 1700 nm range. The NIR spectrometer can accurately detect 100% LDPE substances.

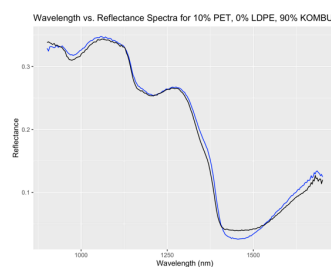


Figure 10: 10% PET, 0% LDPE, 90% KOMBU best fits the spectra graph of: 0% PET, 0% LDPE, 100% KOMBU; peak intensity in the 1150 nm range. The spectrometer correctly determined the mixture was mostly KOMBU.

However, for Figures 11, 12, and 13, there were some discrepancies in the matched graphs. For Figure 11, the test composition was 28% PET, 7% LDPE, 65% kombu, but was matched with the composition 0% PET, 0% LDPE, 100% kombu. While there is no exact composition from the first set of trials that matches this test composition from Figure 11, it was expected that the initial composition of 16% PET, 5% LDPE, 79% kombu would produce the closest spectra graph. Even so, it was within the range of expected possibilities because the kombu in the test graph occupied 65% (a vast

majority) of the mass in the sample and the associated composition had a kombu percentage of 100%. However, in Figures 12 and 13, there were more unexpected errors. In Figure 12, the test composition of 79% PET, 21% LDPE, 0% kombu was paired with 0% PET, 100% LDPE, and 0% kombu, and in Figure 13, the test composition of 100% PET, 0% LDPE, 0% KOMBU was matched with 0% PET, 100% LDPE, 0% kombu. In each of these instances, the entire sample was filled with one material, but that single material was incorrectly identified with the least squares algorithm.

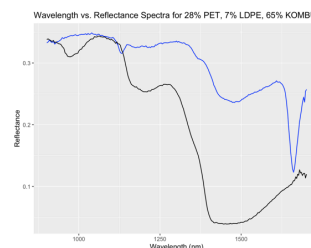


Figure 11: 28% PET, 7% LDPE, 65% KOMBU best fits the spectra graph of: 0% PET, 0% LDPE, 100% KOMBU; peak intensity in the 1150 nm range. The spectrometer inaccurately determined the contents of the 28% PET, 7% LDPE, 65% KOMBU substance.

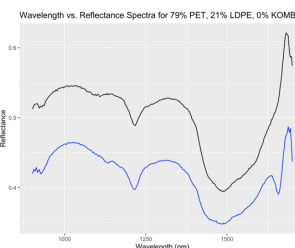


Figure 12: 79% PET, 21% LDPE, 0% KOMBU best fits the spectra graph of: 0% PET, 100% LDPE, 0% KOMBU; peak intensity in the 1700 nm range. The spectrometer inaccurately determined the contents of the 79% PET, 21% LDPE substance.

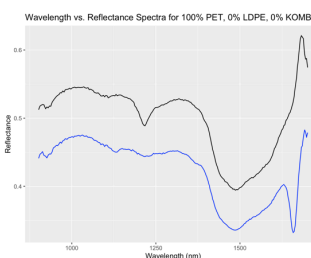


Figure 13: 100% PET, 0% LDPE, 0% KOMBU best fits the spectra graph of: 0% PET, 100% LDPE, 0% KOMBU; peak intensity in the 1700 nm range. The spectrometer inaccurately determined the contents of the 100% PET substance.

There are two main reasons for these false identifications. The first and largest error is that there were not enough trials conducted. Since each composition was tested once in each set of trials, there were probably inaccuracies in the reflectance percentages received for certain wavelengths. Therefore, in the future, many more trials will be conducted for each mass composition and the average spectra values will be taken in order to minimize any false identifications due to errors. Furthermore, more spectra for diverse sample compositions will be obtained. The second reason for the error is because of the least squares method in the algorithm. In particular, Figure 14 shows the spectra graph of 100% PET, 0% LDPE, 0% kombu, with the shredded small pieces, from the second set of trials compared with the spectra graph of 100% PET, 0% LDPE, 0% kombu, with the full uncut pieces, from the first set of trials (this difference in material size in the first versus second dataset is also a small reason for these discrepancies). Even these two graphs were not matched by the least squares

algorithm because the overall distance between the two graphs was not the smallest, yet the graphs appear more identical in terms of their shape (relative minima and maxima, rates of change). Similarly, in Figure 15, while the two graphs that had the most similar mass composition were not matched together, their overall shapes are more similar than the associated match in Figure 13. One reason behind this is because in the samples from the second set of trials, the samples were composed of various small pieces; as such, there were gaps between them and not as much light of each wavelength was reflected back in comparison to their counterparts from the first set of trials. Therefore, one crucial addition to the algorithm will be to compare the relative extrema and rates of change in various sections of the two graphs, using derivatives, in addition to comparing the distance between them.

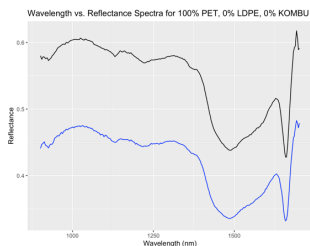


Figure 14: 100% PET, 0% LDPE, 0% KOMBU compared to the spectra graph of: 100% PET, 0% LDPE, 0% KOMBU; peak intensity in the 1700 nm range. The spectrometer accurately detected but misaligned the graph for 100% PET, 0% LDPE, 0% KOMBU.

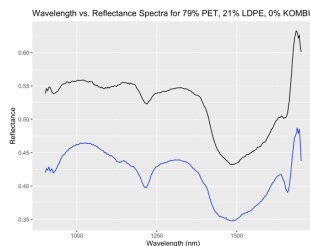


Figure 15: 79% PET, 21% LDPE, 0% KOMBU compared to the spectra graph of: 75% PET, 25% LDPE, 0% KOMBU; peak intensity in the 1700 nm range. The spectrometer accurately detected but misaligned the graph for 79% PET, 21% LDPE, 0% KOMBU.

In future experimentation, these errors will be limited to confirm that NIR spectroscopy is a valid method of detecting microplastics compared to existing methods, namely those that use the Beer-Lambert Law.

Future Research:

The following topics should be further researched and developed: the process through which factory systems physically sort plastic after detection, a system to separate kombu into smaller bits so kombu cannot clog up the conveyor belt, and more cost-effective materials to build a submarine. One key addition that will be incorporated into the algorithm is machine learning, especially once more trials of the experiment are conducted and the number of compositions for which data is collected is increased. In this case, machine learning will be key to sort through the large amounts of data and identify trends that can be used to compare different compositions' spectra. With machine learning, identifying the corresponding graphs will be faster, causing the drone to detect microplastics with elevated accuracy.

Additionally, sonar detection can be implemented to detect microplastics in waters that are not rich in microplastics.⁷ If added, the drones can help clean all the waters at various depths compared to the current drones that are deployed in ocean garbage patches to clean up the rich microplastic density there. Sonar detection does not have an impact on human activity, so long as high frequency transducers are used so humans and marine species cannot hear the sound.⁸ The

sonar transducer would be a part of the outer hull, where it would fire at a fixed angle to cover the most water.⁹ A sonar-proof casing will protect the transducer from the ocean whilst letting sonar frequencies enter and leave. A coding program will be implemented where if the sonar transducer obtains a signal from an object, the boat will be positioned so the current pushes the micro-objects into the PVC pipe and it will use the existing methods to determine whether the micro-objects were microplastics or not.

Conclusion

The results showed that least squares analysis was an overall effective method to compare such spectra graphs and deduce the mass composition of a given sample. However, there were errors in the experiment regarding half of the test cases, as the samples in Figures 11, 12, and 13 were not correctly identified. More improvements including the analysis of the spectra graph's curvature and an increased amount of data are necessary to make the algorithm more accurate.

Acknowledgements

We thank the following individuals for their support and time: Mr. George Epstein; Dr. Christine Leo. We offer our sincere appreciation for their exceptional guidance throughout our project.

References

1. Moore, C. J.; Moore, S. L.; Leecaster, M. K.; Weisberg, S. B. https://ftp.sccwrp.org/pub/download/DOCUMENTS/AnnualReports/1999AnnualReport/10_ar11.pdf (accessed Oct 11, 2021).
2. Long, M.; Moriceau, B.; Gallinari, M.; Lambert, C.; Huvet, A.; Raffray, J.; Soudant, P. Interactions between microplastics and phytoplankton aggregates: Impact on their respective fates. <https://www.sciencedirect.com/science/article/abs/pii/S0304420315000766> (accessed Oct 11, 2021).
3. Allen, L. How satellites and machine learning are being used to detect plastic in the Ocean. <https://www.forbes.com/sites/alenelizabeth/2020/04/27/how-satellites-and-machine-learning-are-being-used-to-detect-plastic-in-the-ocean/?sh=240a9fb64fd1> (accessed Oct 11, 2021).
4. Nicolas Coca, P. D. Classical least squares method for quantitative spectral analysis with python. <https://towardsdatascience.com/classical-least-squares-method-for-quantitative-spectral-analysis-with-python-1926473a802c> (accessed Oct 11, 2021).
5. Corradini, F.; Bartholomeus, H.; Lwanga, E. H.; Gertsen, H.; Geisen, V. Predicting soil microplastic concentration using vis-nir spectroscopy. <https://www.sciencedirect.com/science/article/pii/S0048969718335435> (accessed Oct 11, 2021).
6. Zhu, S.; Chen, H.; Wang, M.; Guo, X.; Lei, Y.; Jin, G. Plastic solid waste identification system based on near infrared spectroscopy in combination with support Vector Machine. <https://www.sciencedirect.com/science/article/pii/S2542504818300113> (accessed Oct 11, 2021).
7. Galceran, E.; Djapic, V.; Carreras, M.; Williams, D. P. A Real-time Underwater Object Detection Algorithm for Multi-beam Forward Looking Sonar. http://robots.engin.umich.edu/~egalcera/papers/galceran_ngcuv2012.pdf (accessed Oct 11, 2021).
8. Active sonar - springer. https://link.springer.com/chapter/10.1007/978-0-387-30441-0_96 (accessed Oct 11, 2021).
9. Selecting a sonar transducer. <https://www.westmarine.com/WestAdvisor/Selecting-a-Sonar-Transducer> (accessed Oct 11, 2021).
10. Pelletier, M. J. (n.d.). Quantitative Analysis Using Ra

man Spectrometry. <https://journals.sagepub.com/doi/pdf/10.1366/000370203321165133>. Retrieved February 17, 2022, from https://journals.sagepub.com/doi/full/10.1366/000370203321165133?url_ver=Z39.88-2003&url_id=ori%3Arid%3Aacrossref.org&url_dat=cr_pub++0pubmed
<https://doi.org/10.1152/ajplung.00306.2018>

■ Authors

Brandon Pae is a senior from the Horace Mann School who wants to protect the environment through technology. As such, he has created a company, Cypol Technologies, with Darson Chen to clean up the oceans with plastic-collecting drones. In college, he plans to study environmental engineering.

Darson Chen is a senior from the Horace Mann school who passionately studies nanoparticles, nanotechnology, and environmental issues. He co-founded Cypol Technologies, designed plastic-collecting drones, and wrote papers detailing nanotechnology's method to combat plastic pollution in the future. In college, he plans to study material science and engineering.